Climate Scientists Misapplied Basic Physics — A Synopsis

A mistake in the climate model architecture changes everything—heat trapped by extra carbon dioxide just reroutes to space from water vapor

Dr David M.W. Evans[1]

November 2015 — this update 17 February 2016

Project home: sciencespeak.com/climate-basic.html

See the Summary for a shorter version (13 pages).

Dr David Evans earned six degrees related to modeling and applied mathematics over ten years, including a PhD from Stanford University. He was instrumental in building the carbon accounting system Australia uses to estimate carbon changes in its biosphere, for the Australian Greenhouse Office.

Abstract

The scientists who believe in the carbon dioxide theory of global warming do so essentially because of the application of "basic physics" to climate, by a model that is ubiquitous and traditional in climate science. This model is rarely named, but is sometimes referred to as the "forcing-feedback framework/paradigm." Explicitly called the "forcing-feedback model" (FFM) here, this pen-and-paper model estimates the sensitivity of the global temperature to increasing carbon dioxide.

The FFM has serious architectural errors. It contains crucial features dating back to the very first model in 1896, when the greenhouse effect was not properly understood. Fixing the architecture, while keeping the physics, shows that future warming due to carbon dioxide will be a fifth to a tenth of current official estimates. Less than 20% of the global warming since 1973 was due to increasing carbon dioxide.

Increasing carbon dioxide "thickens the blanket", reducing the heat radiated to space by carbon dioxide. In reality, the blocked heat mainly just reroutes out to space by being radiated from water vapor instead, all in the upper atmosphere. In the current climate models, however, that blocked heat travels down to the Earth's surface where it is treated like extra sunlight, and instead *less* heat is radiated to space from water vapor.

[1] david.evans@sciencespeak.com, sciencespeak.com

The belief in the danger of increasing carbon dioxide is wholly due to a poor modeling assumption made over a century ago. This error presumably went unnoticed because critics focused on the values of the parameter values in the model (such as how much heat is trapped by increasing CO_2) rather than on how the model combines them (the architecture).

1 Introduction

This document summarizes a series of blog posts where this work debuted for public scrutiny. The blog posts are based on a scientific paper, currently undergoing peer review.

1.1 Significance of the Forcing-Feedback Model (FFM)

This document focuses on the forcing-feedback model (FFM) of climate. It is the conventional sensitivity model for estimating the Earth's sensitivity to CO_2. Predating computer simulations, it is the application of "basic physics" to the climate.

The idea that "it's the physics" makes the CO_2 theory impregnable in the minds of many. They remain convinced that increasing carbon dioxide causes dangerous warming essentially because of the FFM, rather than because of the huge opaque computer models. They are so convinced by the FFM that, for them, it overrides empirical evidence—discordant empirical evidence is presumed to be somehow wrong.

The FFM ignited concern about carbon dioxide; without it we probably wouldn't be too worried. The Charney Report of 1979, the seminal document that ushered in the current era of concern about carbon dioxide, presents the FFM as its first of three arguments. The FFM is ubiquitous in climate science, embedded in the conversation. Its ideas underlie all of establishment climate science; it's the basic mental model, so pervasive that one might overlook it because it is everywhere. One can construct the FFM just from what "everyone knows" in climate science. Yet it does not have a formal name, perhaps because it has been omnipresent for decades, since the birth of modern climate science. Here we've called it the "forcing-feedback model" (FFM) so it can be discussed explicitly.

There is no empirical evidence that rising levels of carbon dioxide will raise the temperature of the Earth's surface as fast as the UN's Intergovernmental Panel on Climate Change (IPCC) predicts. The predictions are entirely based on calculations with models.

Hence a necessary (though not sufficient) condition for overturning the CO_2 theory is that the FFM be invalidated.

1.2 Road Map

The FFM consists of three parameter values, and an architecture that ties them together. Until now critics have almost exclusively queried the parameter values, but here we accept all the conventional parameter values in [IPCC, 2013] (AR5). Examining the architecture, we find two major flaws. We modify the architecture of the FFM to fix those flaws. Fitting climate data to the alternative sensitivity model finds that the sensitivity to CO_2 is an order of magnitude lower than estimated by the FFM and the IPCC. The alternative model also resolves the empirical data over the tropical hotspot.

2 Energy Balance

In basic models of climate, the incoming energy is equal to the outgoing energy. Thus they are only for the transition of Earth from one steady-state to another, and can only be applied between endpoints that are assumed close to steady state.

A variable (e.g. X) in the initial steady-state has a "0" subscript (e.g. X_0), while the change from the initial to the final steady-state is prefixed with a "Δ" (e.g. ΔX). In steady state the outgoing long-wave radiation (OLR) R matches the absorbed solar radiation (ASR) A,

$$A = R, \tag{1}$$

in what is known as "energy balance" or "radiation balance" (both are ~239 W m^{-2}). Thus

$$\Delta A = \Delta R. \tag{2}$$

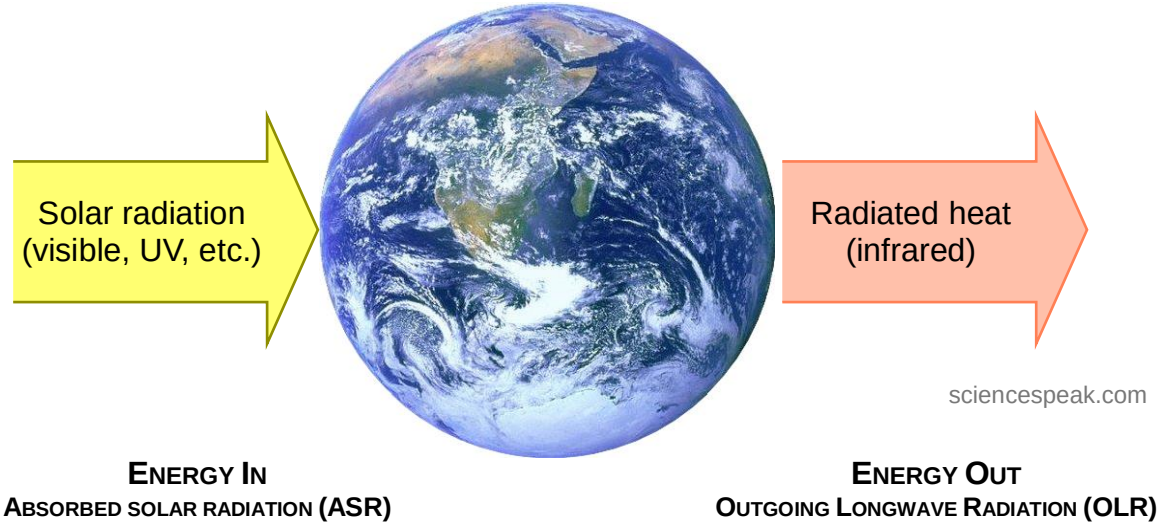

Figure 1: In steady state, ASR equals OLR.

3 The Forcing-Feedback Model (FFM)

3.1 The Three Parameters

3.1.1 The Decrease in OLR from Carbon Dioxide when CO_2 Doubles

An increasing atmospheric concentration of CO_2 reduces the amount of OLR emitted by CO_2, by an amount proportional to the base-2 logarithm L of the CO_2 concentration C. The decrease in OLR emitted by CO_2 molecules per doubling of the CO_2 concentration, when everything else is held constant, is (AR5, p. 8SM-7)

$$D_{R,2X} = -\frac{\partial R}{\partial L} = 3.7\,[3.5, 4.1]\ \mathrm{W\,m^{-2}}. \tag{3}$$

3.1.2 The Planck Sensitivity

The increase in the average surface temperature of the Earth T_S as the net downward flux from the top of the atmosphere increases, but everything else is held constant, is

$$\lambda_0 = \frac{1}{\partial R/\partial T_S} \simeq \frac{1}{3.2 \pm 0.1} = 0.31 \pm 0.01 \ ^\circ\mathrm{C\,W^{-1}\,m^2}, \tag{4}$$

where the value of its reciprocal is $3.2 \pm 0.1\ \mathrm{W\,m^{-2}\,^\circ C^{-1}}$ (AR5, p. 818) (which is the increase in OLR as the surface warms, called the "Planck feedback", though it is not really a feedback because it does not affect what causes it). The business of "holding everything constant" is slightly arbitrary, so it is deemed to be the Planck conditions—namely that all else besides mean tropospheric temperatures and OLR are held constant, there are no feedbacks, all tropospheric temperatures (including the surface temperature) move in unison, and stratospheric temperatures are unchanged [Soden & Held, 2006, pp. 3355-56].

3.1.3 The Total Feedback

The increase in net downward flux from the top of the atmosphere in response to surface warming is the total feedback

$$f = 1.7\,[0.97, 2.43]\ \mathrm{W\,m^{-2}\,^\circ C^{-1}}. \tag{5}$$

AR5 (Table 9.5 and Fig. 9.43, and p. 591) reports the individual and total feedbacks from the CMIP5, in $\mathrm{W\,m^{-2}\,^\circ C^{-1}}$: water vapor +1.6±0.3, lapse rate −0.6±0.4, water vapor and lapse rate combined +1.1±0.2, surface albedo +0.3±0.1, cloud +0.3±0.7.

Later we partition the feedbacks into those that affect albedo (f_α , all the surface albedo and some of the cloud feedbacks), and those that do not ($f_{\bar{\alpha}}$):

$$\begin{aligned} f &= f_\alpha + f_{\bar{\alpha}} \\ f_\alpha &= 0.4 \pm 0.5\ \mathrm{W\,m^{-2}\,^\circ C^{-1}} \\ f_{\bar{\alpha}} &= 1.3 \pm 0.5\ \mathrm{W\,m^{-2}\,^\circ C^{-1}}. \end{aligned} \tag{6}$$

3.2 The Architecture

The FFM is just a radiation balance. (It is derived here and here, based on the leading climate textbook and a paper by leading climate theorists.) The radiation imbalances ("forcings") caused by the various climate drivers are calculated, and then added to form the total radiative imbalance. Then the model calculates the surface warming required to increase the OLR by just enough to restore the radiation to balance, after taking the feedbacks to surface warming into account. The model architecture is shown in Fig. 2.

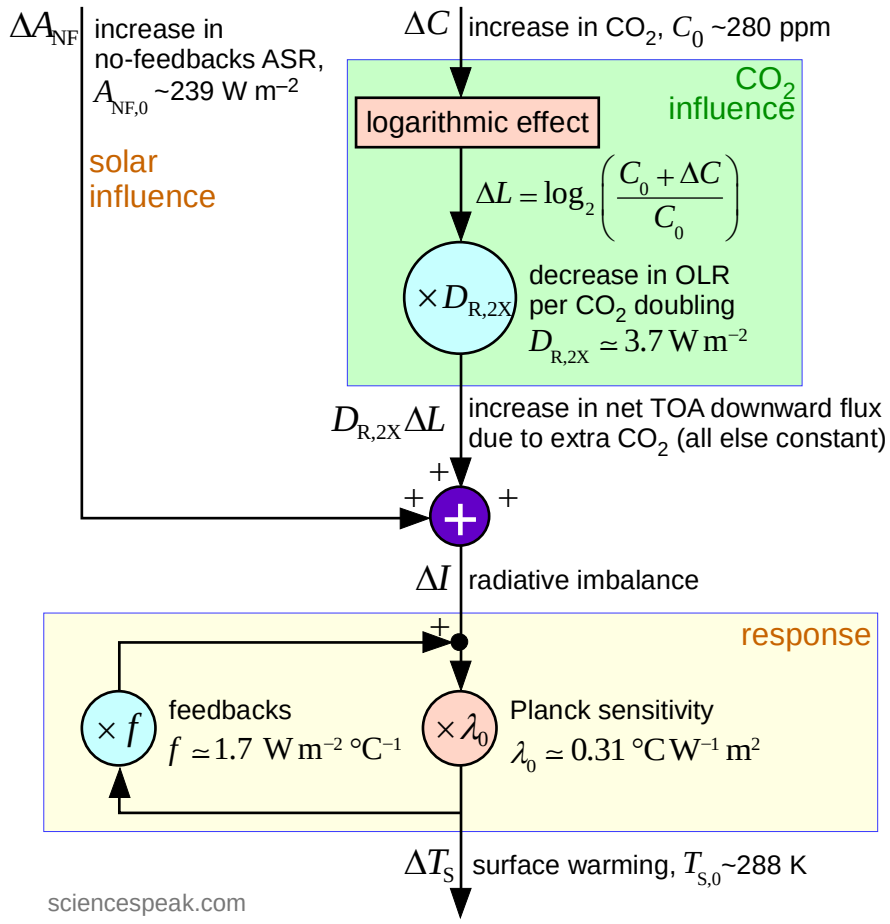

Figure 2: The forcing-feedback model (FFM) of climate, for the two main drivers: increased ASR (other than due to feedbacks in response to surface warming) and increased CO_2.

The surface warming, by inspection of Fig. 2, is

$$\Delta T_S = \Delta I \lambda_0 \left[1 + f\lambda_0 + (f\lambda_0)^2 + \ldots\right] = \frac{\lambda_0}{1 - f\lambda_0}\Delta I = \frac{\lambda_0}{1 - f\lambda_0}\left(\Delta A_{NF} + D_{R,2X}\Delta L\right). \qquad (7)$$

3.3 Estimating the ECS

The ECS is the surface warming when the CO_2 concentration doubles (i.e. ΔL is one) and other drivers are unchanged:

$$\mathrm{ECS} = \frac{\lambda_0}{1 - f\lambda_0} D_{R,2X} = \frac{D_{R,2X}}{\lambda_0^{-1} - f} \simeq \frac{3.7\,[3.5, 4.1]}{3.2 \pm 0.1 - 1.7\,[0.97, 2.43]} \simeq 2.5[1.24, 3.7]\ \mathrm{°C}. \qquad (8)$$

This accords with AR5 (p. 1033, p.1451–2), which finds the ECS as likely to be 1.5°C to 4.5°C for a doubling of equivalent CO_2 concentration. Setting f to zero in Eq. (8) gives the no-feedbacks-ECS, namely $1.16[1.08, 1.29]$ °C.

3.4 Major Architectural Errors

3.4.1 Omits Feedbacks other than to Surface Warming

The architecture in Fig. 2 only includes feedbacks in response to surface warming. If there exists a feedback which responds to a climate driver, but is not triggered by some other driver or the surface warming it causes, then there is literally no place for it in the conventional ar-

chitecture—it is omitted. A feedback that is specific to a particular climate driver would not be triggered by other climate drivers or by the surface warming they caused, so such a feedback is *not* a response to surface warming.

3.4.2 Solar Response Applied to all Climate Drivers

The architecture in Fig. 2 summarizes the effect of all the various climate drivers in a single number, the radiative imbalance ΔI. Thus, as far as the calculation of surface warming is concerned, any climate driver is interchangeable with any other climate driver that produces the same radiative imbalance (forcing).

The model treats the radiative imbalance due to any climate driver by the identical response, namely the Planck sensitivity coupled with feedbacks to surface warming—multiplication by $\lambda_0/(1-f\lambda_0)$. The Planck sensitivity is the surface warming associated with a change in OLR or ASR while everything about the climate is kept constant, then the feedbacks allow everything to change in response to the surface warming. Hence the response that is applied to all the climate drivers is the "solar response"—the surface warming for an increase in ASR (ΔA_{NF} to be more precise), in °C per W m^{-2}.

The "CO_2 response", the surface warming due to an increase in CO_2 forcing in °C per W m^{-2}, is quite distinct from the solar response:

Response to More ASR (the "solar response")	Response to More CO_2 (the "CO_2 response")
Increases OLR	OLR unchanged[2] (redistributes OLR between emitters)
Adds energy to the climate system	Blocks energy from leaving the climate system
Occurs mainly at the surface	Occurs mainly in the upper troposphere

Table 1: The differences between the solar and CO_2 responses are substantial.

While a decrease in heat outflow is equivalent to a matching increase in heat inflow in terms of the amount of heat on the planet, it is not necessarily equivalent in terms of how the outgoing heat is distributed between the various emitters (water vapor, CO_2, cloud tops, the surface, etc.). Surface warming is determined only by the change in emissions from the surface—because a hotter surface emits more to space.

The assumption: *the surface warming due to increased CO_2 is the same as the surface warming due to the increased absorbed sunlight that causes the same forcing.* This was a convenient assumption because it made the problem of estimating sensitivity to CO_2 tractable—the effect of extra absorbed sunlight could be estimated, in large part by the Stefan-Boltzmann equation. Notice that this assumption is intrinsic to the architecture of the FFM (Fig. 2). It seems *especially* unlikely to be true given that the total emitted heat is different.

The FFM applies the solar response to the influence of increased CO_2—but how realistic can that be? Not very, it turns out, as we show using modern climate data.

[2] Ignoring the minor effect of surface albedo feedback in response to surface warming.

4 The Rerouting Feedback

The "rerouting feedback" is proposed. It is a feedback that is specifically in response to increased CO_2; it is part of the CO_2 response but is not a response to surface warming.

4.1 The Feedback

Increasing the CO_2 concentration warms the upper troposphere, because the emissions spectrum changes and there is more warming by downward emissions from the extra CO_2. (See the changing OLR spectrum in this last diagram on this page of Barrett-Bellamy and compare it to the blackbody radiance temperatures drawn on an observed emission spectrum such as from Nimbus.) See Fig. 10.

This heats neighboring molecules, including water vapor molecules in the water vapor emissions layer (WVEL) and some cloud tops, so more OLR is emitted by water vapor molecules and cloud tops. (The WVEL is the optical top band of water molecules that can emit to space—upwards emissions by water vapor molecules beneath the top layer are absorbed by water vapor molecules higher up. While usually in the upper troposphere, it moves up and down as water vapor moves within the atmosphere.) See Fig. 12.

The WVEL emits more so it must be at a higher average temperature, due to a combination of warming by increased CO_2 and a decline in average height moving it to a warmer altitude.

4.2 Causes the WVEL to Descend

How does increased CO_2 affect the average height of the WVEL? Atmospheric water vapor is dynamic, so a possible mechanism involves meteorology. (In contrast, CO_2 is relatively static and well-mixed, so radiative concerns are usually sufficient to explain its behavior.)

Upper tropospheric warming by increased CO_2 distorts the local lapse rate, which becomes less steep (less cooling per km of rise). The atmosphere around the WVEL altitude becomes warmer and more stable. The moist air rising by convection thus rises less vigorously and not as high, and so the average height of the WVEL declines. Because increasing CO_2 lowers the vigor of convection in the upper troposphere, humidity builds up and clouds condense at lower levels, suggesting the average height of the cloud tops declines.

This explanation of the lowering of the WVEL by the rerouting feedback relies only on the altered movements of water vapor due to increased CO_2, rather than on radiation transfer.

4.3 Comments

It is called the "rerouting feedback" because some fraction of the OLR that is blocked by rising CO_2 levels from escaping to space from CO_2 molecules is *rerouted* to space via emission from water vapor and cloud tops instead.

This rerouting takes place high in the atmosphere, far from the surface, so there is no place for it in the FFM—it is in the blindspot of that model, which contains only feedbacks in response to surface warming.

The heat rerouted to space via water vapor molecules is not available to travel down and warm the surface, as in the conventional models. Thus the rerouting feedback reduces the im-

pact of increasing CO_2 on surface warming. If this feedback is real and significant, it could help explain why CO_2 is not as potent as the IPCC supposes. See Fig.s 10, 11, and 12.

5 The Alternative Sensitivity Model

5.1 Fixes

Forming the alternative sensitivity climate model by fixing the architecture of the FFM requires two changes. We also make two optional improvements.

5.1.1 Each Climate Driver Needs its own Specific Feedbacks and Response

The appropriate response must be applied to the forcing due to each climate driver. So a driver-specific response, including any driver-specific feedbacks, calculates the surface warming ("warming") due to that driver. The warmings thus calculated are added together to form the total surface warming, because the climate is approximately linear for the small temperature perturbations involved in global warming—the effects of a driver on other drivers are assumed to be second order. The CO_2 response is assumed proportional to CO_2 forcing, so the response is to multiply the CO_2 forcing by the CO_2 sensitivity λ_C.

This solves both major architectural errors in the FFM. Note the paradigm shift: the conventional model adds forcings, while the alternative model adds warmings.

5.1.2 Retaining the Radiation Balance

Radiation must balance (Eq. (2)), but this is no longer guaranteed merely by the connections in the model. However radiation balance in the model is ensured by setting the increase in ASR ΔA, where it occurs in that model, equal to the increase in OLR ΔR, which must be obtained by some other means.

ΔA is the increase in no-feedbacks-ASR, ΔA_{NF}, plus the increase in albedo in response to surface warming, namely $f_\alpha \Delta T_S$ (Eq. (6)), so the model must explicitly form that sum. This leaves just the non-albedo feedbacks $f_{\bar{\alpha}}$ in the feedback loop inside the solar response.

5.1.3 Replace the Planck Sensitivity with the Stefan-Boltzmann Sensitivity (Optional)

The Planck sensitivity only applies under the Planck conditions, which are technically impossible because climate feedbacks cannot be held constant (thus the Planck sensitivity is not empirically verifiable). It is preferable to avoid this quantity.

The Stefan-Boltzmann equation applied to the Earth defines a quantity T_R such that

$$R = \sigma \varepsilon T_R^4, \tag{9}$$

where σ is the Stefan-Boltzmann constant (5.67×10^{-8} W m^{-2} K^{-4}) and ε is the Earth's emissivity (~0.995). This being the Stefan-Boltzmann equation, T_R is a temperature (~255 K), which we call the "radiating temperature". While the Stefan-Boltzmann law cannot be literally applied to Earth because there is no solid, uniform, isothermal surface that emits all the OLR, this definition of T_R effectively applies it. Assuming ε is constant, T_R is a proxy for OLR. T_R may be thought of as the OLR converted to a temperature, or as some sort of average of the temperatures of the various emissions layers.

T_R is numerically similar to the Earth's effective temperature T_e, the temperature of a *black* body that emits the same OLR as the Earth: R equals σT_e^4, so T_e is $\varepsilon^{1/4} T_R$ or ~$0.999 T_R$. The numerical difference between T_R and T_e is insignificant, but here we are concerned with OLR from the real Earth so it is more natural to use radiating temperature.

The Stefan-Boltzmann sensitivity (SBS) is defined as the slope of the T_R curve as a function of R in the Earth's current neighborhood, found by differentiating in Eq. (9):

$$\lambda_{SB} = \frac{dT_R}{dR} = \frac{1}{4\sigma\varepsilon T_R^3} = \frac{T_R}{4R} \simeq \frac{255}{4\times 239} = 0.267 \text{ °C W}^{-1}\text{ m}^2. \tag{10}$$

The SBS is the ratio of ΔT_R to the corresponding ΔR, in all circumstances. It is the slope of the Stefan-Boltzmann curve at the Earth's current state; it is regarded here as a constant, because the Earth does not stray far from this point—the effect of a change in λ_{SB} is second-order in the modeling here.

The Planck sensitivity is ~17% greater than the Stefan-Boltzmann sensitivity, mainly because under the Planck conditions the stratospheric temperatures are held constant as the surface warms, so the OLR from stratospheric CO_2 and ozone does not change.

5.1.4 Separate Inputs for EDA and TSI (Optional)

A change in externally-driven albedo (EDA) is a change in albedo that is not attributable to feedbacks in response to surface warming. Empirical evidence and a simple proportional variation argument suggests that the effect of changes in EDA on surface warming is at least twice as great as the direct effect of changes in TSI, and possibly much more. EDA is omitted from conventional climate models.

5.2 The Sum of Warmings Sub-Model

Applying the four fixes above to the FFM of Fig. 2 produces the sum-of-warmings model in Fig. 3.

Except for the CO_2 sensitivity, the parameter values in the sum-of-warmings model can all be calculated from the conventional model. Comparing the solar response in Fig. 3 to the (solar) response in Fig. 2, and noting that M is the in-line form of the non-albedo feedbacks to surface warming due to more ASR,

$$\frac{\lambda_0}{1 - f_\alpha \lambda_0} = M \lambda_{SB} \tag{11}$$

so M is ~2.0.

The alternative and conventional sensitivity models differ by only one connection: if the CO_2 forcing $D_{R,2X}\Delta L$ in Fig. 3 is disconnected from the CO_2 response and instead added to the node that adds ΔA_{NF} to $f_\alpha \Delta T_S$, then Fig. 3 becomes the same model as in Fig. 2. Hence the alternative and conventional models are fundamentally different—they cannot both be correct (unless the CO_2 and solar responses are equally strong, that is, λ_C equals $M\lambda_{SB}$).

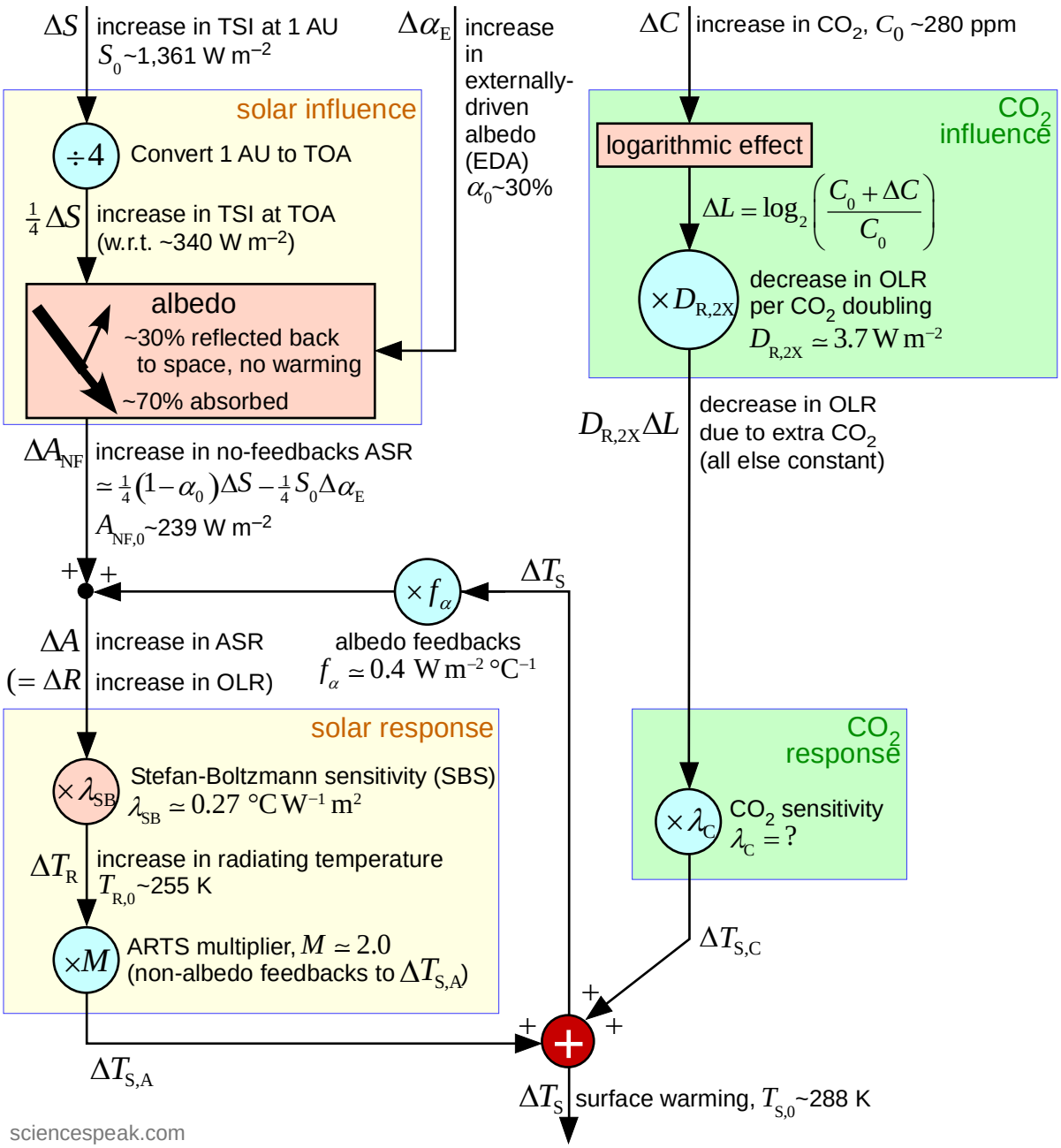

Figure 3: The sum-of-warmings model of climate. The alternative sensitivity model combines this model and an OLR model, by setting the increase in ASR here equal to the increase in OLR computed by the OLR model.

5.3 The OLR Sub-Model

The alternative model needs an estimate of the increase in OLR, for radiation balance. The increase in OLR over an observed period is estimated using an OLR model whose inputs are the changes in the parameters of the main emissions layers. This drags a lot more data into the calculation of the sensitivity to CO_2, but it is perhaps the simplest way of determining the actual OLR, or at least bounding it. The OLR model is in this spreadsheet, and is developed here, here, here, and here.

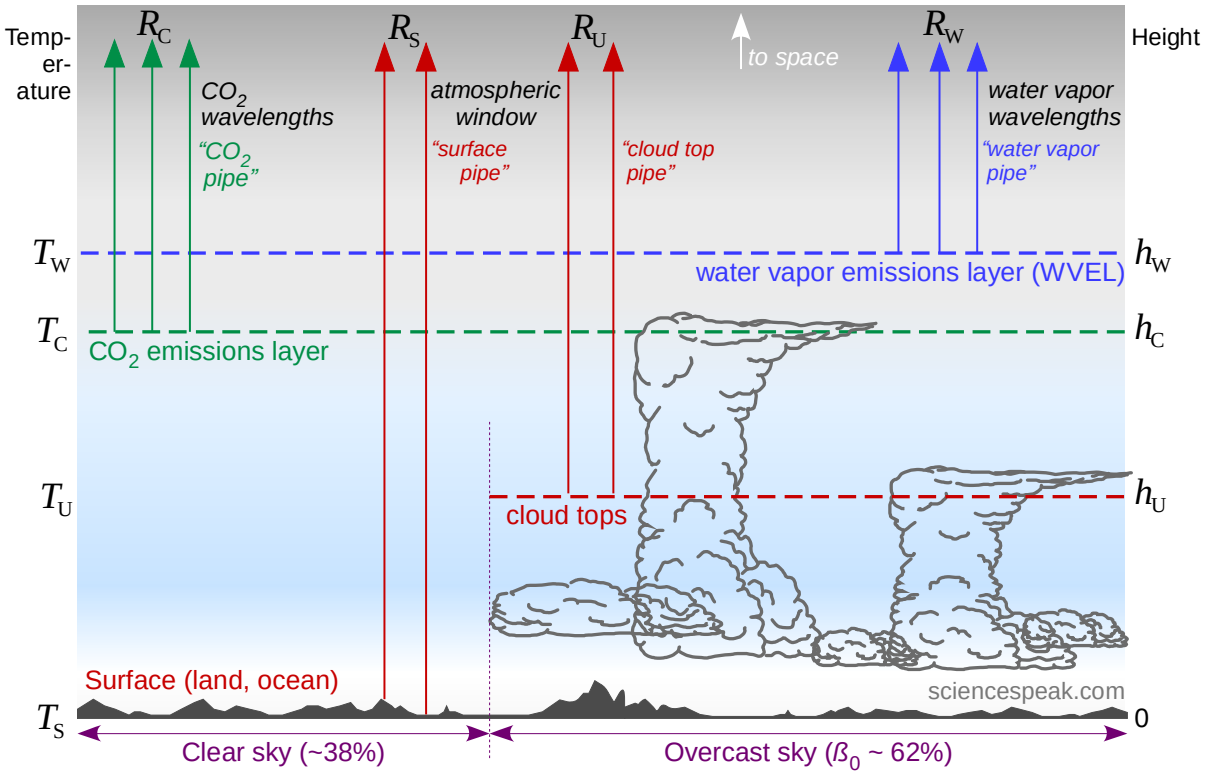

Figure 4: The OLR model estimates the change in OLR from properties of the main emission layers. (Although the CO_2 emissions layer is in the stratosphere around the center of its blockage at 15 µm, averaging by wavelength across the whole CO_2 blockage gives an average height around 7 km, out in the wings of the blockage, which also happens to be where the main changes due to increasing CO_2 are occurring. Hence this depiction.)

The increase in OLR is modeled as

$$\Delta R = \tau \Delta T_S + \theta_W \Delta h_W + \theta_U \Delta h_U + g \Delta \Gamma + D_\beta \Delta \beta + \theta_M \Delta h_M - D_{R,2X} \Delta L \tag{12}$$

where

- h_W, h_U, and h_M are the average heights of the WVEL, the cloud tops, and the methane emission layer, respectively; $h_{W,0} \simeq 8\,\text{km}$, $h_{U,0} \simeq 3.3\,\text{km}$, $h_{M,0} \simeq 3\,\text{km}$
- Γ is the average lapse rate; $\Gamma_0 \simeq 6.5\ °\text{C km}^{-1}$
- β is the cloud fraction; $\beta_0 \simeq 62\%$

and

$$\begin{aligned}
\tau &\simeq 3.2\ \text{W m}^{-2}\ °\text{C}^{-1} \\
\theta_W &\simeq -8.7\ \text{W m}^{-2}\ \text{km}^{-1} \\
\theta_U &\simeq -4.6\ \text{W m}^{-2}\ \text{km}^{-1} \\
g &\simeq \begin{cases} -13.5\ \text{W m}^{-2}\ \text{per}\ °\text{C km}^{-1} & \text{uniform} \\ -9.4\ \text{W m}^{-2}\ \text{per}\ °\text{C km}^{-1} & \text{partial} \end{cases} \\
D_\beta &\simeq -0.42\ \text{W m}^{-2}\ \text{per}\ 1\% \\
\theta_M &\simeq -0.5\ \text{W m}^{-2}\ \text{km}^{-1}.
\end{aligned} \tag{13}$$

The value of g depends on whether the lapse rate is assumed to change uniformly across the troposphere (the conventional assumption) or only in the lower 5 km (in line with radiosonde data). Note that τ is $\partial R/\partial T_S$; its value agrees with the Planck feedback from AR5 (Eq. (4)).

The parameter values in this model come from the climate literature, the ratio of areas on an Nimbus emission spectrum over the tropical Pacific Ocean, or elementary calculations about lapse rate and Stefan-Boltzmann surfaces. They are for average OLR, heights, and temperatures of the main emissions layers, averaged over area, time of day and year, and applicable wavelengths. What follows is not terribly sensitive to these parameters.

The data in OLR datasets isn't good enough for our purposes. The OLR dataset at NOAA from 1974 reads low, and gridding and interpolation lower its resolution too far. The CERES global OLR dataset from 2000 is better, but the period is too short. A major advantage to using the OLR model is that it gives a lot of insight into what is going on.

5.4 The Alterative Model

From the sum-of-warmings model, add the warmings due to ASR and CO_2:

$$\Delta T_S = \Delta T_{S,A} + \Delta T_{S,C} = M\lambda_{SB}\Delta A + \lambda_C D_{R,2X}\Delta L\,. \tag{14}$$

Form the alternative model by using the OLR model (Eq. (12)) and energy balance (Eq. (2)) to replace ΔA:

$$\omega\Delta T_S = \theta_W\Delta h_W + \theta_U\Delta h_U + g\Delta\Gamma + D_\beta\Delta\beta + \theta_M\Delta h_M + \left(\frac{\lambda_C}{M\lambda_{SB}} - 1\right)D_{R,2X}\Delta L \tag{15}$$

where

$$\omega = \frac{1}{M\lambda_{SB}} - \tau \simeq -1.34\ \mathrm{W\,m^{-2}\,{}^\circ C^{-1}}. \tag{16}$$

Hence, for a period between two steady states, the estimate of CO_2 sensitivity is

$$\lambda_C = M\lambda_{SB}\left[\frac{\omega\Delta T_S - \left(\theta_W\Delta h_W + \theta_U\Delta h_U + g\Delta\Gamma + D_\beta\Delta\beta + \theta_M\Delta h_M\right)}{D_{R,2X}\Delta L} + 1\right]. \tag{17}$$

Then the fraction of global warming due to extra CO_2 can be estimated as

$$\mu = \frac{\Delta T_{S,C}}{\Delta T_S} = \frac{\lambda_C D_{R,2X}\Delta L}{\Delta T_S}, \tag{18}$$

and the ECS as

$$\mathrm{ECS} = \Delta T_{S,C}\big|_{\Delta L=1} = \lambda_C D_{R,2X}\,. \tag{19}$$

6 The Missing Hotspot

The water vapor emissions layer (WVEL) plays a crucial role in climate. The WVEL is the top band of the water vapor, around one optical depth as seen from space on the wavelengths at which water vapor absorbs and emits. It is, on average, where OLR is typically emitted by water vapor molecules. Upwards emissions by water vapor molecules beneath the WVEL are generally absorbed by water vapor molecules higher up. The WVEL is fairly dynamic, rising and falling as water vapor is moved around the atmosphere, but on average it is in the upper troposphere. If it ascends (that is, its average height Δh_W increases) then it cools and emits less OLR. Its average height is ~8 km, though in the tropics it is ~10 km.

6.1 The Hotspot is Caused by an Ascending WVEL

The "hotspot" is the informal name for a warming of the upper troposphere, in the tropics. The air above the WVEL is dry, but the air below the WVEL is moist and therefore warmer because water vapor is condensing and releasing its latent heat. If the WVEL ascends it creates the hotspot, which is the warming of a volume that was dry and cool when just above the WVEL but which becomes moist and warmer as the WVEL ascends above it.

6.2 When the WVEL Ascends

Surface warming causes more evaporation (70% of the surface is ocean), and the greater volume of water vapor in the atmosphere is presumed to push up the WVEL. This causes the WVEL to cool and emit less OLR, so the other emitters must emit more than otherwise to compensate, including the surface. For the surface to emit more it must warm. This mechanism, called "water vapor amplification" because any surface warming is amplified by the ascent of the WVEL, creates the hotspot.

The main effect of the solar response is to warm the surface, so it also causes the WVEL to ascend. In the FFM all climate drivers cause the solar response, so surface warming due to any climate driver causes the WVEL to ascend, water vapor amplification, and a hotspot. (While more complicated, the GCMs do essentially the same—see Fig.s 6 and 7 below.)

6.3 The WVEL Has Not Ascended in the Last Few Decades

The only instruments with sufficient vertical resolution to measure the change in height of the WVEL over the last few decades are the radiosondes. Satellites are not suitable because they aggregate information from several vertical kilometers into each data point.

6.3.1 Temperature Data

The temperatures measured by the radiosondes for 1979 to 1999 are shown in Fig. 5 (the only image as a function of height and latitude ever publicly released, apparently).

Over those two decades, the atmosphere at the WVEL height of ~8 km warmed by ~0.12 °C per decade due to surface warming (midpoints of UAH and HadCrut4, 5-year smoothed) and a further 0.04 ± 0.03 °C per decade due to lapse rate changes in response to surface warming. But the observed warming in Fig. 5 was only ~0.1 °C per decade. Subtracting out the warming that is simply due to surface warming and lapse rate changes, what is left are the temperature changes for other reasons—namely no change or perhaps a slight cooling around 8 to 10 km in the tropics. This is not compatible with an ascending WVEL.

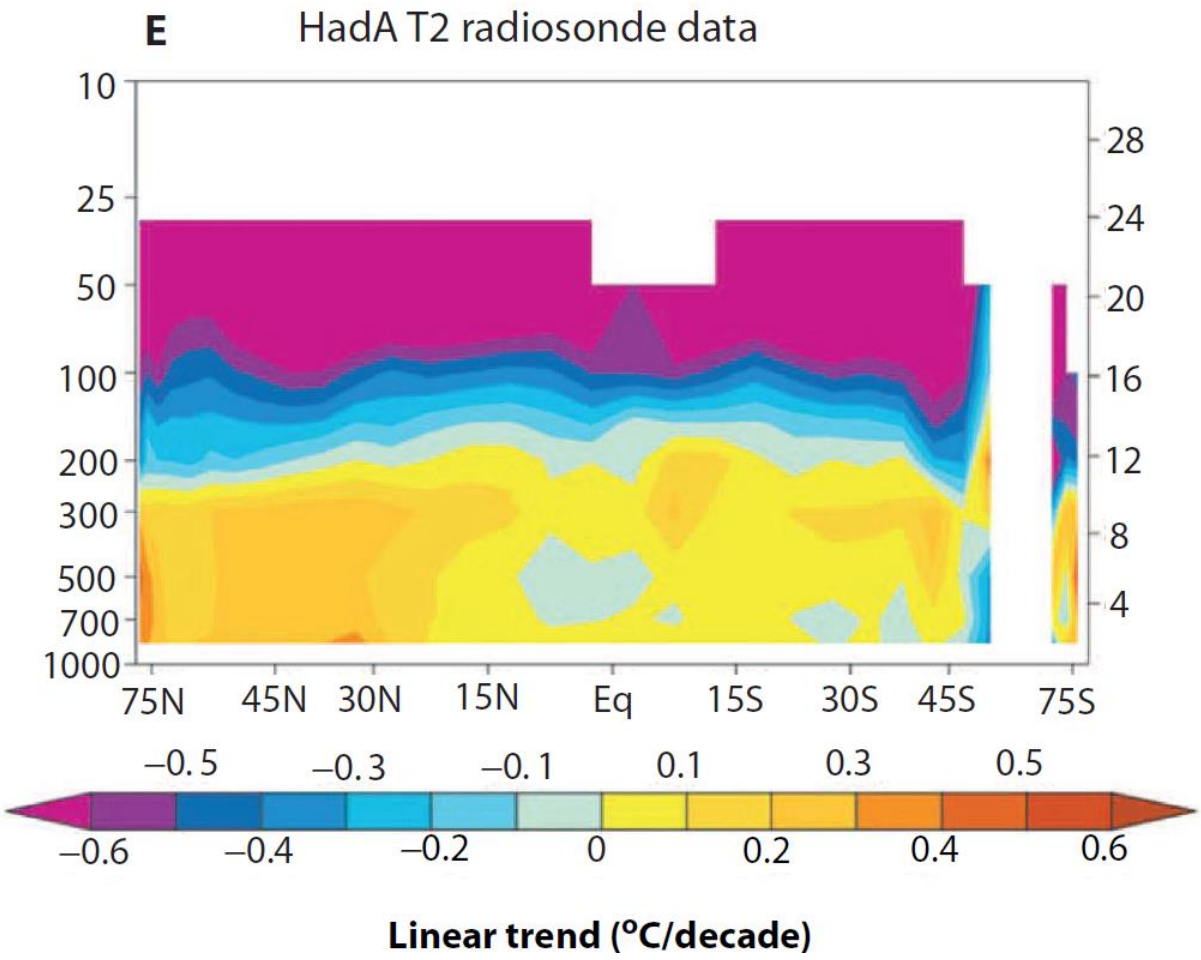

Figure 5: Atmospheric warming 1979 to 1999, as measured by the radiosondes. The horizontal axis shows latitude, the vertical axis height (km on the right, hPa on the left). From the US CCSP report of 2006, Fig. 5.7E in section 5.5 on page 116 [Santer, 2006]. The CO_2 concentration increased 9% (or 13% of a doubling).

Dr Roy Spencer, who pioneered microwave sounding for measuring atmospheric temperatures from satellites, used a different mix of microwave channels to specifically look for the hotspot using the satellite data in May 2015. He concluded: "But I am increasingly convinced that the hotspot really has gone missing. ... I believe the missing hotspot is indirect evidence that upper tropospheric water vapor is not increasing, and so upper tropospheric water vapor (the most important layer for water vapor feedback) is not amplifying warming from increasing CO_2."

The cooling strips above 12 km are due to ozone depletion, too high to be of interest here.

Compare Fig. 5 with outputs from a prototypical GCM, the GISS Climate Model E:

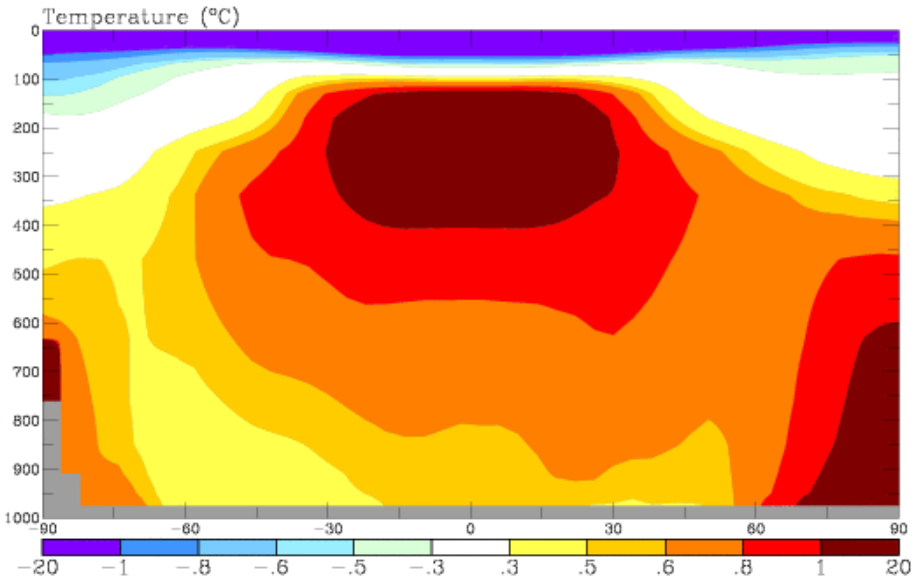

Figure 6: Atmospheric warming when the CO_2 concentration increases by 25% (or 32% of a doubling) with no change in solar irradiance, as predicted by the GISS Climate Model E. The prominent warming over the tropics at about 10 km (250 hPa, vertical scale) is the hotspot. Compare to reality for 13% of a CO_2 doubling, in Fig. 5.

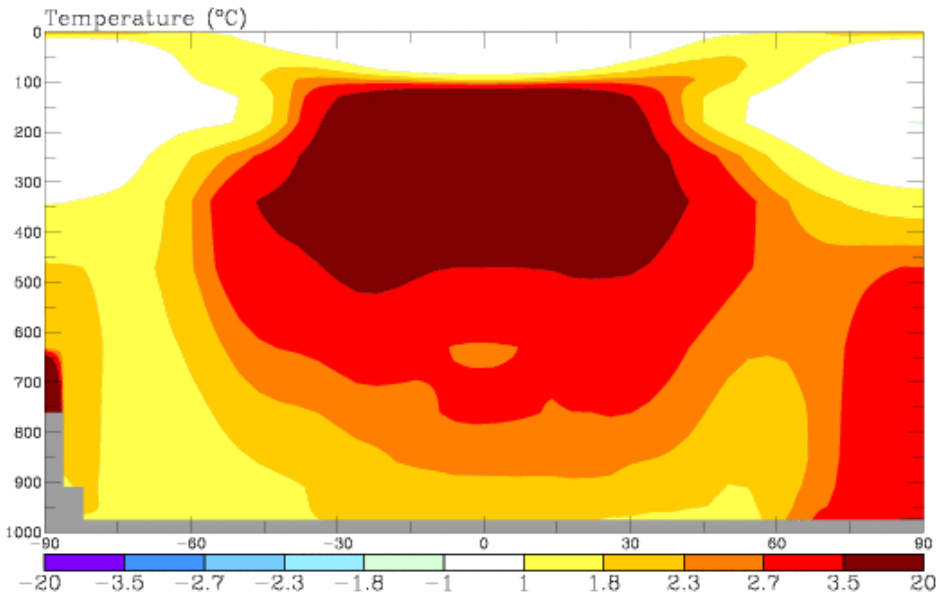

Figure 7: Atmospheric warming when the solar irradiance increases by 2% but CO_2 is held constant, as predicted by the GISS Climate Model E. Compare to its prediction for 32% of a CO_2 doubling in Fig. 6—while the amount of warming is different. the pattern is similar. This shows that this GCM applies roughly the same feedbacks to a solar forcing as a CO_2 forcing, in particular the water vapor amplification of surface warming.

Fig.s 6 and 7 are clearly nothing like Fig. 5. Supporters of the conventional models explain away this clash by ignoring or disputing the radiosonde data, and substituting vague satellite data instead—even though satellites, due to inadequate vertical resolution, are the wrong tool for the job. For example, see here or here or here. A simpler explanation, that accords with Fig. 5, lies in improved architecture: don't apply the solar response to the influence of CO_2.

6.3.2 Humidity Data

Consider the specific humidity data from the radiosondes, shown in Fig. 8. It must be treated with great caution, particularly at altitudes above the 500 hPa pressure level—following the

discussion in [Paltridge, Arking, & Pook, 2009], the humidity data is restricted to tropical and mid-latitude data at least ~0.5 g/kg, from 1973. The more reliable data only goes to the 400 hPa altitude level, but above 500 hPa the trend is one of drying. The same trends are shown by the earlier radiosonde data from 1948 to 1973. Like the temperature data, this is not compatible with an ascending WVEL.

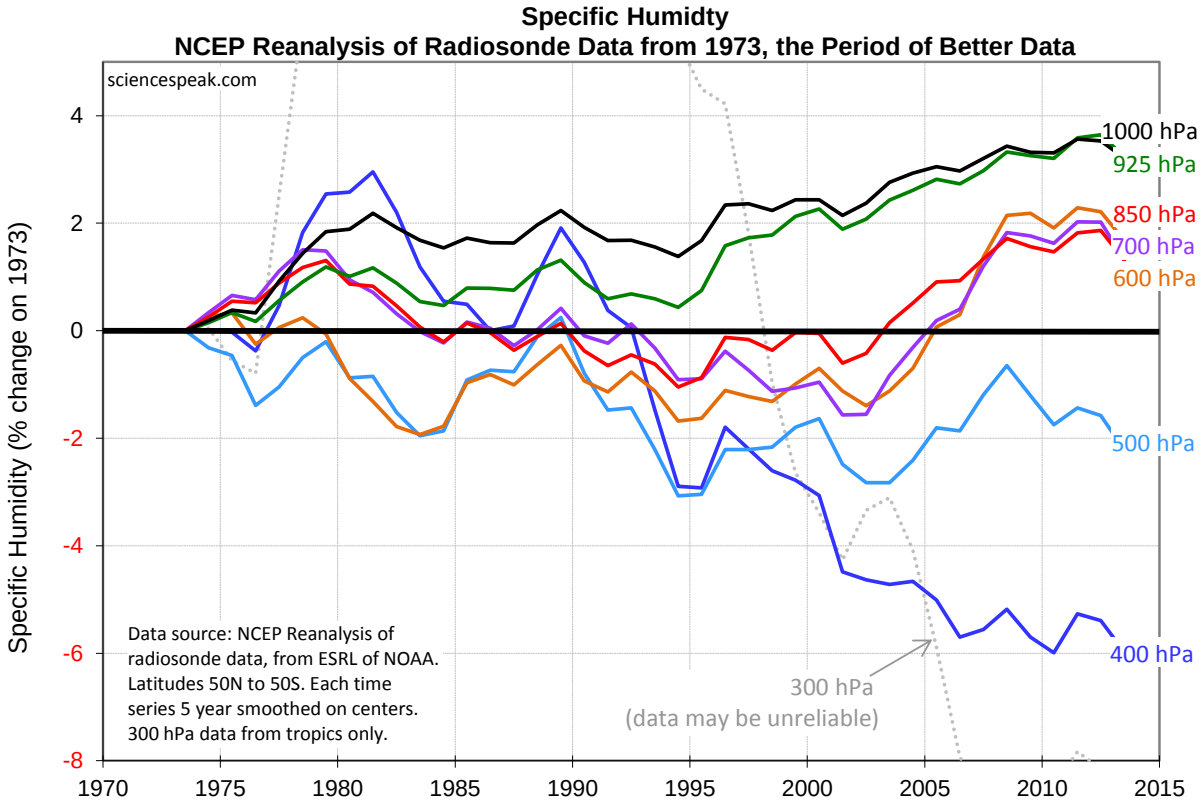

Figure 8: The atmosphere near the average WVEL height of 360 hPa shows a drying trend since 1973.

6.3.3 Conclusion

While the data is not good enough to estimate changes in the average height of the WVEL, it is sufficient to distinguish the direction of movement—not up.

$$\Delta h_{\mathrm{W}} \leq 0\,. \tag{20}$$

6.4 The CO2 Response Causes the WVEL to Descend

Since 1973 the world has seen changes in two main climate influences:

- An increase in solar forcing, mainly due to externally driven albedo (EDA). This triggered the solar response, which caused the WVEL to ascend.
- An increase in CO_2 forcing, which caused the CO_2 response. This caused surface warming, which in turn caused the WVEL to ascend. It *also* caused the CO_2-specific feedbacks (which include the rerouting feedback, which lowers the WVEL).

The WVEL moved down in this period. Therefore:

- The CO_2-specific feedbacks caused the WVEL to descend, outweighing the ascent due to the combination of CO_2-induced surface warming and the solar response.
- The CO_2 response caused the WVEL to descend.
- The GCMs, which predict strong water vapor amplification and a rise in the WVEL in response to *both* increased solar forcing and increased CO_2 forcing, are incorrect.

6.5 Pictorial

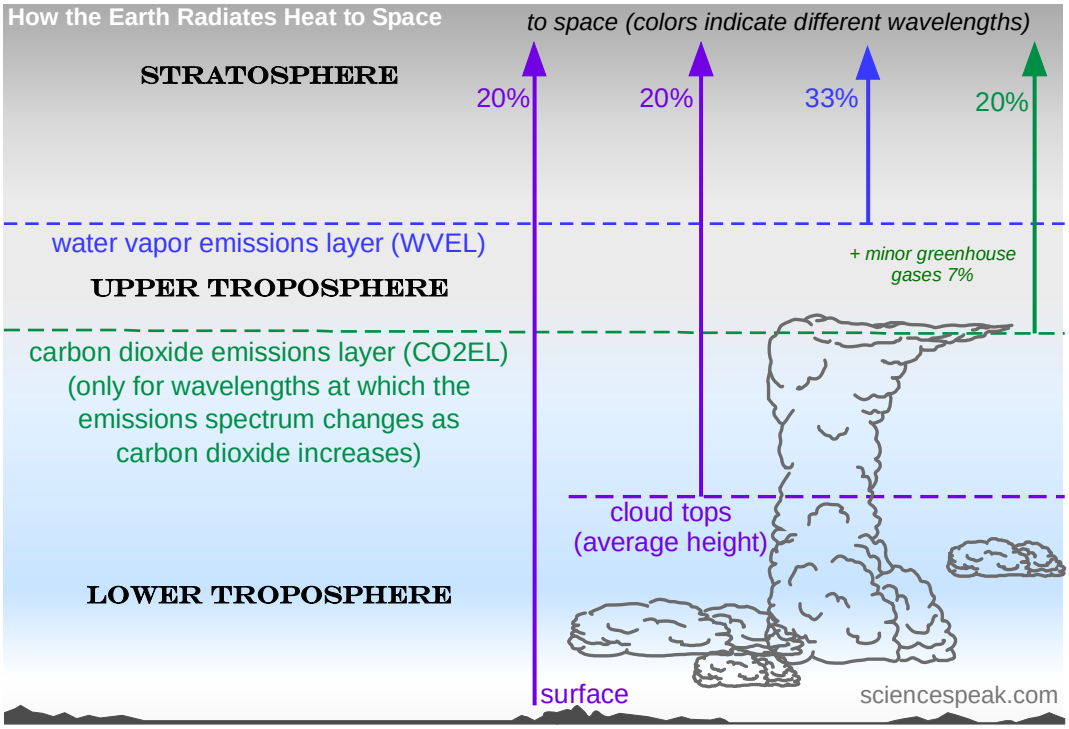

Figure 9: How the Earth radiates heat to space.

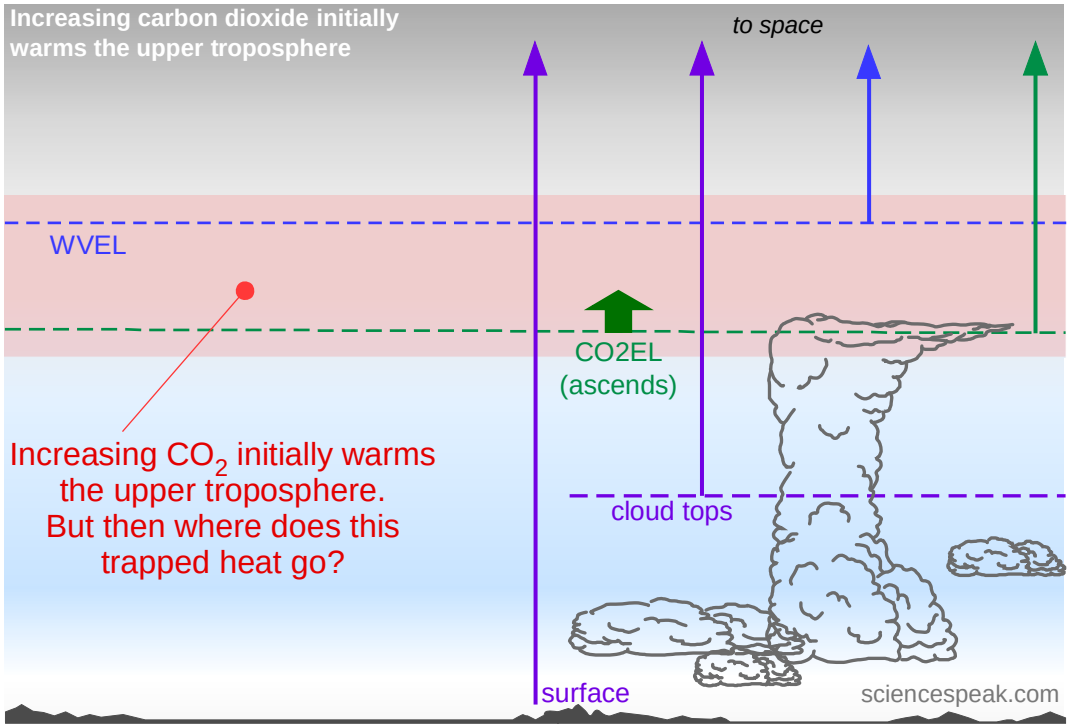

Figure 10: Increasing CO_2 initially warms the upper troposphere. But what happens to that trapped heat next?

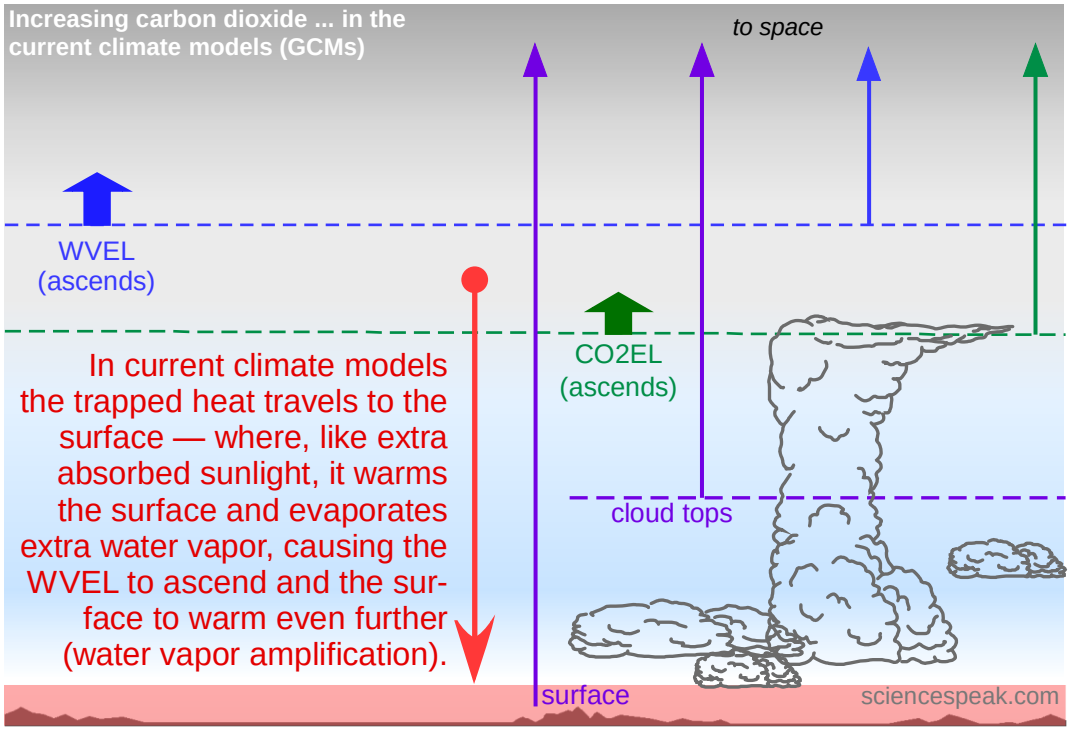

Figure 11: When CO_2 is increasing, the current climate models (GCMs) move the trapped heat to the surface.

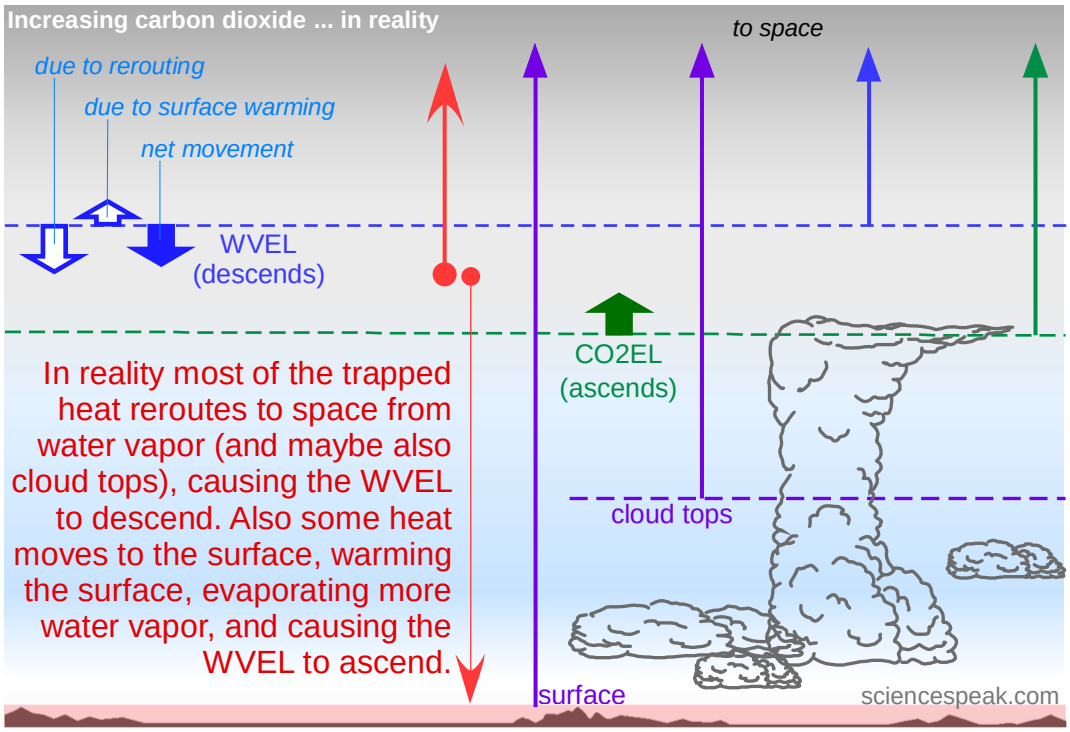

Figure 12: When CO_2 is increasing, most of the trapped heat simply reroutes to space from water vapor molecules and perhaps also the cloud tops, and only a little moves to the surface. (As deduced in Fig. 14.)

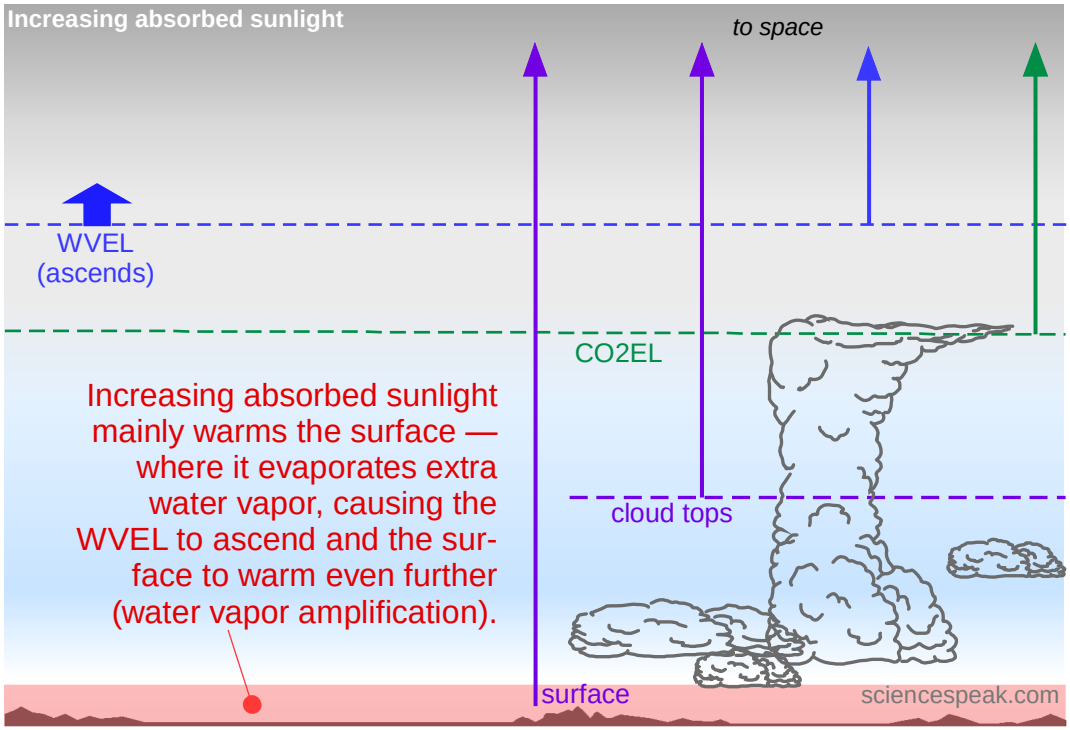

Figure 13: When absorbed sunlight is increased, the surface warms.

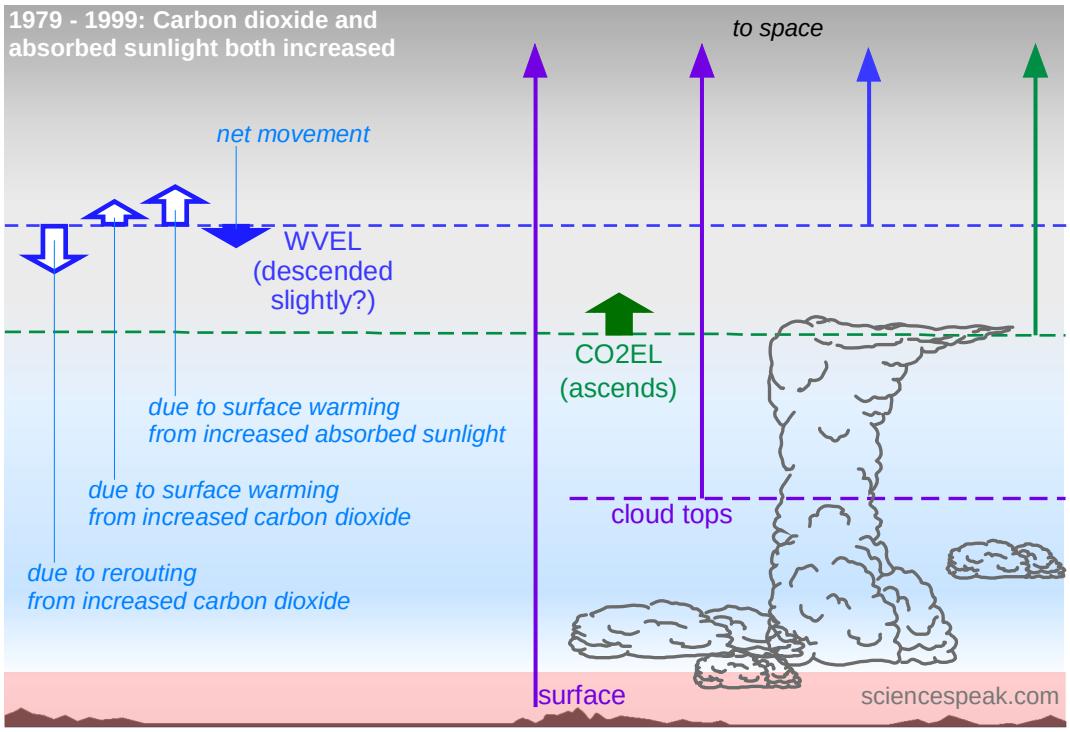

Figure 14: The period 1979 to 1999 saw considerable surface warming during a period of increasing CO_2 and increasing absorbed sunlight (predominately due to decreasing albedo), yet the WVEL did not ascend (as evidenced by the missing hotspot). This suggests that the increasing CO_2 caused only a small portion of the surface warming because most of the trapped heat was rerouted to space (Fig. 12) rather than moved to the surface (Fig. 11), while the increasing absorbed sunlight caused the bulk of the surface warming (Fig. 13). The increasing CO_2 lowered the WVEL, while simultaneously the increasing absorbed sunlight lowered the WVEL, for a net effect on the WVEL of nothing or maybe a small descent.

7 Effect of Increasing Carbon Dioxide

The climate data is insufficient to form good estimates, but is sufficient to draw interesting conclusions. The data about the climate parameters are considered below, and then various combinations of parameter values are evaluated in "scenarios". The numerical calculations are all in this spreadsheet.

7.1.1 Cloud Height

[Davies & Molloy, 2012] report a decrease in the global effective height of cloud tops from March 2000 to February 2010, using the Multiangle Imaging SpectroRadiometer (MISR) on the Terra satellite. The linear trend was of −44 ± 22 m/decade; the difference between the first and last years was −31 ± 11 m. The annual mean height is measured with a sampling error of 8 m. Detected regional height anomalies correlate well with changes in the Southern Oscillation Index.

However [Evan & Norris, 2012] claim that the decrease reported by the MISR is an artifact due to a systematic reduction in the number of retrievals of clouds at lower elevations during the early years of the MISR mission, apparently due to "satellite orbit inclination maneuvers" causing "erroneous co-registration of the nine MISR cameras". But they also note that "there is no obvious reason why the camera co-registration issues should affect cloud height retrievals at one height in the atmosphere more or less strongly than retrievals at another height in

the atmosphere." Using a post-hoc method for removing the bias, they report an ascending trend of +54 m/decade, which agrees with the MODIS-Terra data showing increasing cloud height of +61 m/decade. The MODIS-Terra cloud height data is of distinctly lesser quality than the MISR for measuring cloud top height; both begin in 2000.

There does not appear to be any other cloud height data of note. Unfortunately the cloud height data is conflicted, and is after the period of warming from the 1970s to the 1990s. We explore both ascending and descending cloud-top scenarios below.

7.1.2 Lapse Rate

The published radiosonde data on lapse rate trends only seems to extend to 700 hPa. Behavior in the upper troposphere might be quite different (Fig. 8). [Gaffen, Santer, Boyle, Christy, Graham, & Ross, 2000] reports that observed surface-to-700-hPa lapse rates fluctuated less than 1.5% either way about an average value from 1960 to 1998, and there might have been no overall trend (the trend might have decreased from 1960 to 1979 then increased from 1979 to 1998).

In lieu of empirical data on changes in lapse rate $\Delta\Gamma$, we estimate it from the lapse rate feedback f_{LR} in AR5. Though this feedback is only for the solar response (Fig. 3), we assume it applies for any surface warming because it is intended as such, the effect is theoretically straightforward, and we have no better information. Assuming a uniformly changing lapse rate as per the conventional model, the extra OLR due to $\Delta\Gamma$ is $-\Delta T_{\mathrm{S}} f_{\mathrm{LR}}$ from the lapse rate feedback while it is $g_{\mathrm{uniform}}\Delta\Gamma$ by the OLR model, so

$$\Delta\Gamma \simeq -\frac{\Delta T_{\mathrm{S}} f_{\mathrm{LR}}}{g_{\mathrm{uniform}}}. \tag{21}$$

To apply this in the alternative model, we assume the lapse rate only changes in the lower troposphere in line with the radiosonde data: the increase in OLR due to lapse rate changes is estimated to be $g_{\mathrm{partial}}\Delta\Gamma$.

7.1.3 Cloud Fraction

The International Satellite Cloud Climatology Project indicates that the cloud fraction rose by ~2% from 1984 to 1987, then fell ~4% to 2000, and then rose ~0.5% to 2010. [Marchand, 2012] reports cloud fraction from 2001 to 2011 as measured by MISR rising ~0.1% and by MODIS-Terra and MODIS-Aqua rising ~0.3%. The total change from 1984 to 2010 was ~−1.5% according to the ISCCP but that is exaggerated by a factor of 2 to 4 by comparison to MISR and MODIS over 2001 to 2011, so perhaps the cloud fraction fell by ~0.5% from 1984 to 2011. There does not seem to be prior data.

7.1.4 Scenarios

Table 2 shows several scenarios. In any scenario, λ_{C}, μ, and the ECS must all be positive, which constrains the input values.

Scenario	Start	End	ΔT_S	ΔC	Δh_W	Δh_U	$\Delta\Gamma$	$\Delta\beta$	Δh_M	λ_C	μ	ECS	ΔR
			°C	ppm	m	m	°C per km	%	m	°C W^{-1} m^2	%	°C	W^{-1} m^2
A4	1973	2011	0.514	62.0	0	0	-0.023	-0.50	0	-0.11	-20	-0.42	1.16
A5	1973	2011	0.444	62.0	0	0	-0.020	-0.25	0	0.02	4	0.07	0.80
A6	1973	2011	0.514	62.0	-25	100	-0.023	-0.50	0	0.03	5	0.11	0.91
A7	1973	2011	0.514	62.0	0	200	-0.023	-0.50	0	0.42	76	1.57	0.23
B4	1948	2011	0.488	81.0	0	0	-0.022	-0.50	0	0.07	18	0.27	0.75
B5	1948	2011	0.488	81.0	0	200	-0.022	-0.50	0	0.47	120	1.75	-0.18
C1	2000	2010	0.045	21.0	0	-42	-0.002	0.20	0	0.19	125	0.71	-0.02
C2	2000	2010	0.045	21.0	0	-20	-0.002	0.20	0	0.38	246	1.39	-0.12
C3	2000	2010	0.045	21.0	0	54	-0.002	0.20	0	0.99	653	3.68	-0.47
C4	2000	2010	0.045	21.0	0	61	-0.002	0.20	0	1.05	691	3.90	-0.50
C5	2000	2010	0.045	21.0	-18	-31	-0.002	0.20	0	0.00	0	0.00	0.08
C6	2000	2010	0.045	21.0	-50	50	-0.002	0.20	0	0.18	115	0.65	-0.01

Table 2: The A and B scenarios match the period of radiosonde data back to 1973 (more reliable) and 1948 (less reliable), during which the radiosondes indicate the WVEL did not ascend. The C scenarios are for the period of cloud-top height data. Surface warming averages UAH and HadCrut4, both 5-year smoothed.

The C scenarios are for 2000 to 2010, where we have cloud-top height data. Suppose the WVEL remained at the same height. If the cloud tops descended between 42 and 20 m as per the MISR observations, the ECS is likely between 0.7 and 1.4 °C, and μ is from 125% to 250% (C1, C2). But if the cloud tops ascended between 54 and 61 m in line with the MODIS observations, then the ECS is ~3.8 °C and μ is ~650% (so high because the CO_2 warming is much larger than the warming that actually occurred, which requires the existence of an unknown cooling influence that does not affect ASR) (C3, C4). The unrealistically high values of μ suggest that the cloud-tops more likely descended than ascended and that the MISR observations are more likely to be correct. If the WVEL descended then estimates of μ and ECS decrease: a MISR-average cloud-top descent of 31 m and a WVEL descent of 18 m requires an ECS of zero (C5). A WVEL descent of ~50 m is required to bring μ down to ~100% if the cloud tops rose ~50 m (C6).

In the A scenarios with the better radiosonde data from 1973 to 2011, there is cloud fraction data from 1984, but no cloud top height data before 2000. If the cloud tops do not ascend (in line with their probable behavior after 2000), the WVEL does not ascend (as per the radiosondes), and the cloud fraction change was ~−0.5% (in line with observations from 1984), then the ECS estimate is negative (A4). The ECS must be positive, so this indicates that on the basis of the most likely changes the ECS is very small, putting no lower bound on the estimate. Perhaps the pre-satellite warming and the cloud fraction change were exaggerated two-fold: this would increase μ to ~4% and the ECS estimate to ~0.07 °C (A5). Even if the cloud tops ascended 100 m (twice the MODIS figures for 2000 to 2010), and the WVEL descended 25 m, λ_C is ~0.03, μ is ~5% and the ECS is ~0.1 °C (A6). If the cloud tops rose by 200 m (difficult to reconcile with the MISR observations, particularly as the clouds tops average only ~3.3 km) and the WVEL did not change, estimates approach the conventional: μ ~76% and ECS ~1.6 °C (A7).

The longest scenarios are the B scenarios, back to 1948 but with less-reliable or missing data. If the WVEL and cloud tops remained at the same heights, and cloud fraction changed by ~−0.5% (the net change observed from 1984 to 2011), then λ_C is ~0.07, μ is ~18%, and the ECS is ~0.27 °C (B4).

7.1.5 Conclusions

There is no strong basis in the data for favoring any scenario in particular, but the A4, A5, A6, and B4 scenarios are the ones that best reflect the input data over longer periods.

Hence we conclude that the basic physics, when the basic climate model's architecture is fixed and modern data applied, shows that:

- The ECS is likely less than 0.25 °C, and most likely less than 0.5 °C.
- The fraction of global warming caused by increasing CO_2 in recent decades, μ, is likely less than 20%.
- The CO_2 sensitivity is less than a third of the solar sensitivity.

Given a non-ascending WVEL, it is difficult to construct a scenario consistent with the observed data in which the influence of CO_2 is greater than this.

8 GCMs have the Same Architectural Errors

The global circulation models (GCMs), the large computer climate models, take many factors into account and are somewhat diverse, but essentially all exhibit the same two architectural flaws as the FFM.

8.1 Omitted Feedback

GCMs can and do include driver-specific feedbacks, such as extra plant growth in response to increased CO_2, but they usually have only a minor effect on the calculated ECS. No GCMs include something like the rerouting feedback that substantially reduces the potency of CO_2, because then they would need drivers other than CO_2 to explain 20th century warming.

8.2 Solar Response Applied to the CO_2 Forcing Feedback

The responses (in °C of surface warming per W m^{-2} of forcing) of different forcings emerge as slightly different in GCMs. The "efficacy" of various forcings can vary by 30% or so. However, the efficacies of the crucial CO_2 and ASR forcings are always similar.

All GCMs apply the water vapor amplification feedback to both CO_2 and ASR, which are both modeled in GCMs as causing a rising WVEL and a hotspot. This is entirely different from the data-driven alternative model, with its CO_2-specific feedbacks that cause the WVEL to fall, and no hotspot.

See the outputs from a prototypical GCM in Fig.s 6 and 7, which both show a similar atmospheric warming pattern because the GCM applies similar feedbacks to both.

8.3 Tailored to Give Roughly the Same Sensitivity to CO_2 as the FFM

The GCMs are bottom-up models that try to produce observable macro trends by modelling masses of minor details; many details are not known exactly, so some scaling and tweaking is necessary. However they are indirectly tailored to calculate broadly the same CO_2 sensitivity as the conventional basic model, as follows:

1. The FFM estimates the ECS as ~2.5 °C (Eq. (8)). But this is an overestimate: fixing the faulty architecture shows that the ECS is less than 0.5 °C.
2. An ECS of ~2.5 °C roughly accounts for observed warming since 1910. To believers in the FFM, this confirms that increasing CO_2 explains 20th century warming.
3. So the GCMs use increasing CO_2 as the dominant driver to reproduce 20th century warming. GCMs that do not succeed in this task are not published (see p. 32 here).

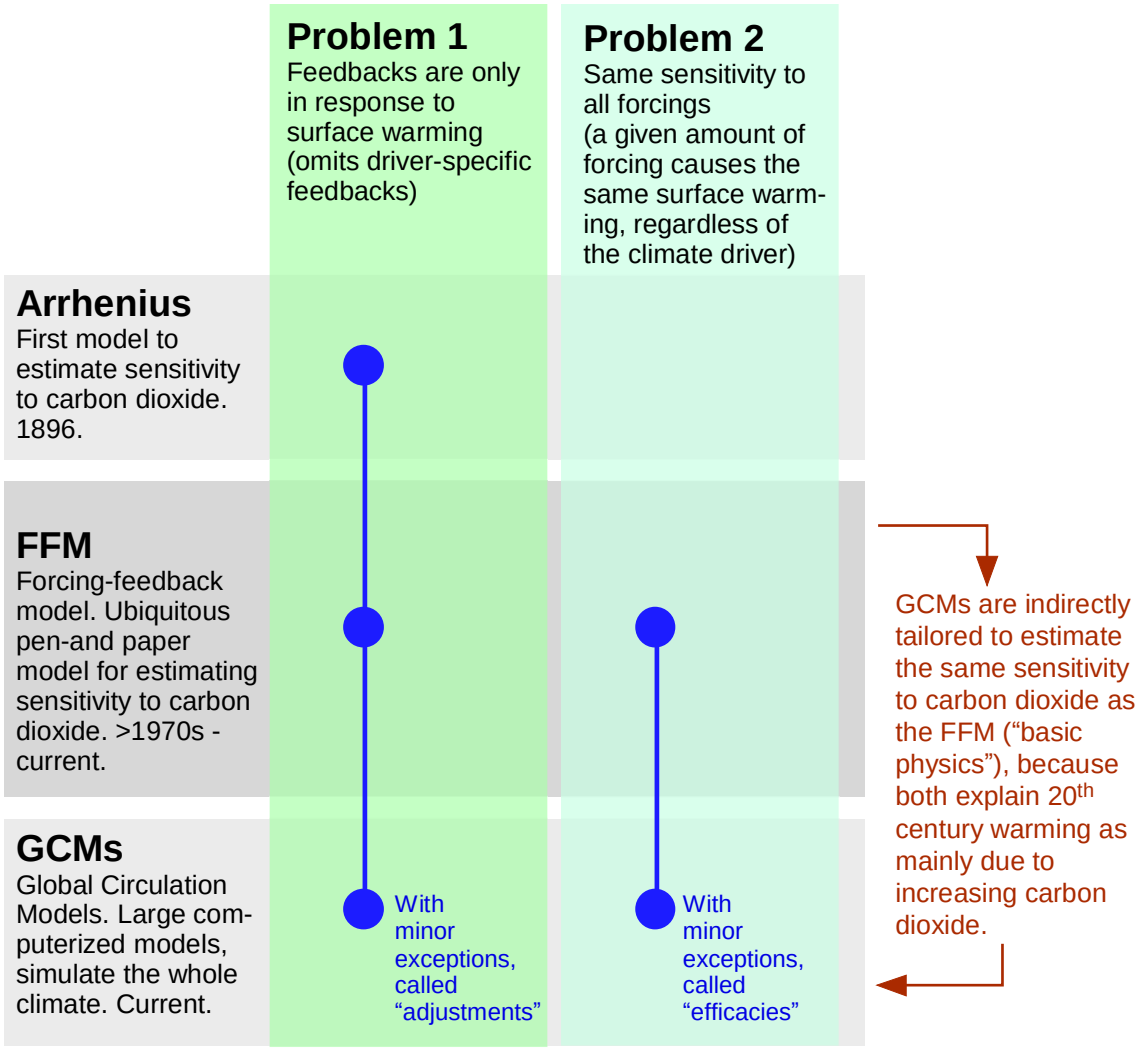

Figure 15: The problems in the development path to the modern climate models. The new sensitivity model in this book, the sum-of-warmings model, is not shown—it's a pen-and-paper model that further refines the FFM and avoids both problems.

9 Conclusion

The conventional forcing-feedback model (FFM) has two major architectural problems that render it invalid: it omits feedbacks that are not in response to surface warming, and it applies the solar response to the radiation imbalance caused by any climate influence. Correcting these flaws requires adding warmings (the surface warmings caused by climate influences in isolation) rather than forcings (the radiation imbalances caused by those climate influences).

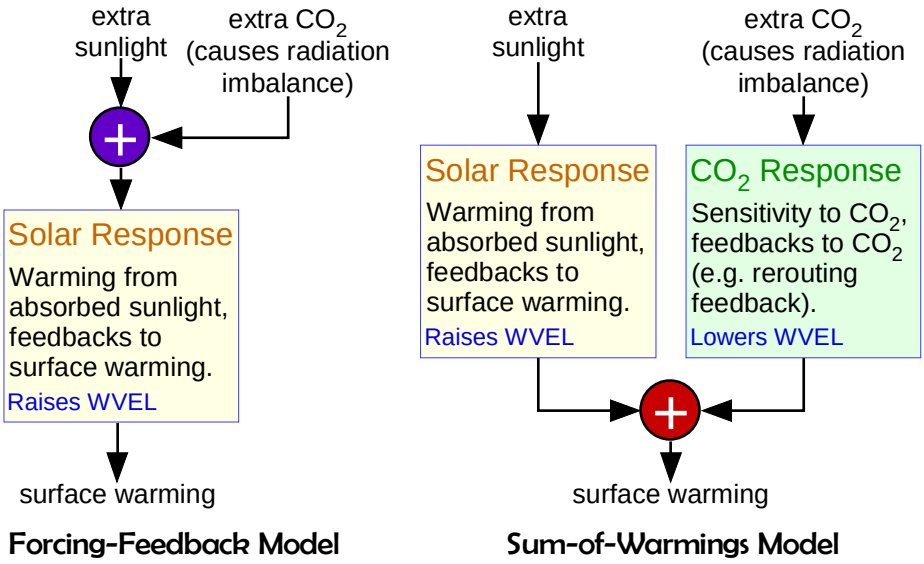

Figure 16: Fixing the architecture by switching from the sum-of-forcings approach of the conventional FFM to a sum-of-warmings finds a much lower sensitivity to CO_2 and resolves the data on water vapor amplification.

Fitting climate data to the new architecture finds that the ECS is an order of magnitude lower than estimated by the FFM. The CO_2-response is less than a third as strong as the solar response, measured in °C of surface warming per W/m^2 of forcing. This is presumably due to the proposed rerouting feedback: increasing CO_2 heats parts of the upper troposphere, causing the WVEL to emit more OLR and thus a lower WVEL.

The FFM, which ignited and guides climate alarm over CO_2, overestimates surface warming due to increasing CO_2 because it applies the strong solar response instead of the weak CO_2 response to the CO_2 forcing.

The new architecture also resolves the data on the water vapor amplification and hotspot: surface warming and the solar response cause water vapor amplification, an ascending WVEL, and the tropical hotspot. However in recent decades this has been slightly outweighed by the lowering of the WVEL due to the rerouting feedback.

Acknowledgements

A big thank-you to numerous readers at the joannenova.com.au blog, for commenting on the series of 19 blog posts in September to November of 2015, for many useful enquiries and suggestions, and for the donations that made this work possible. I am also grateful to Joanne Nova, Garth Paltridge, Christopher Monckton, Frank Hobbs, Andrew McRae, and William Kininmonth for helpful feedback. Thanks also to Michael Hammer (for spectroscopic advice that led to the OLR model) and to Stephen Wilde (for suggesting the rerouting mechanism).

References

Davies, R., & Molloy, M. (2012). Global cloud height fluctuations measured by MISR on Terra from 2000 to 2010. *Geophysical Research Letters*, L03701.

Evan, A. T., & Norris, J. R. (2012). On global changes in effective cloud height. *Geophysical Research Letters*, 39, L19710.

Gaffen, D. J., Santer, B. D., Boyle, J. S., Christy, J. R., Graham, N. E., & Ross, R. J. (2000). Multidecadal Changes in the Vertical Temperature Structure of the Tropical Troposphere. *Science*, Vol 287, 1242-1245.

IPCC. (2013). *Fifth Assessment Report.* Cambridge University Press.

Marchand, R. (2012). Trends in ISCCP, MISR, and MODIS cloud-top-height and optical-depth histograms. *J. Geophys. Res. Atmos.*, 118, doi:10.1002/jgrd.50207.

Paltridge, G., Arking, A., & Pook, M. (2009). Trends in middle- and upper-level tropospheric humidity from NCEP reanalysis data. *Theoretical and Applied Climatology*, 98:351-359.

Santer, B. D. (2006). *US Climate Change Science Program 2006, Temperature Trends in the Lower Atmosphere - Understanding and Reconciling Differences.*

Soden, B. J., & Held, I. M. (2006). An assessment of climate feedbacks in coupled ocean-atmosphere models. *J.Clim.*, 19, 3354-3360.